

Supporting Information

Enhanced surface wettability and innate activity of iron borate catalysts for efficient oxygen evolution and gas bubble detachment

Kamran Dastafkan,^a Yibing Li,^a Yachao Zeng,^a Li Han,*^b and Chuan Zhao*^a

^aSchool of Chemistry, The University of New South Wales, Sydney, New South Wales 2052, Australia

^bSchool of Chemical Engineering and Energy, Zhengzhou University, Zhengzhou 450001, China

* Corresponding author E-mails: lihan@zzu.edu.cn; chuan.zhao@unsw.edu.au

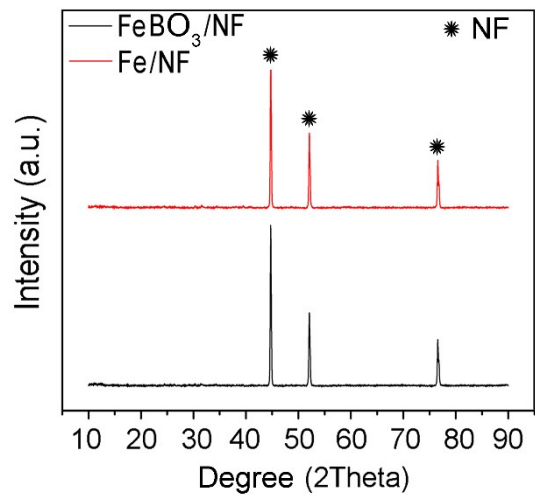


Fig. S1 Comparison between XRD patterns of FeBO_3/NF and Fe/NF samples.

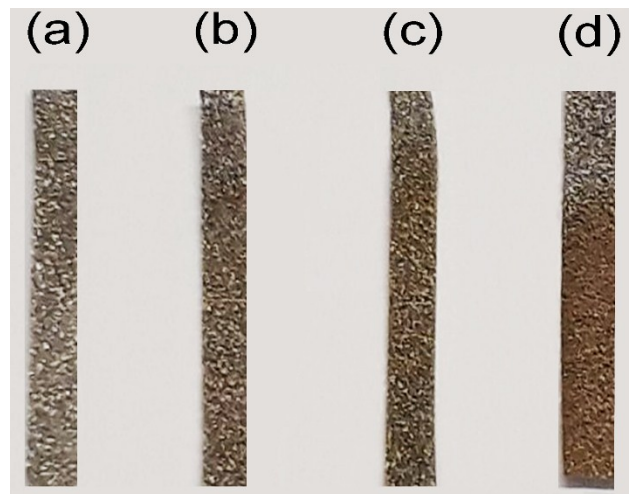


Fig. S2 Images of the prepared (a) pristine NF, (b) $\text{Fe}(\text{OH})_3/\text{NF}$, (c) Fe/NF , and (d) FeBO_3/NF electrodes.

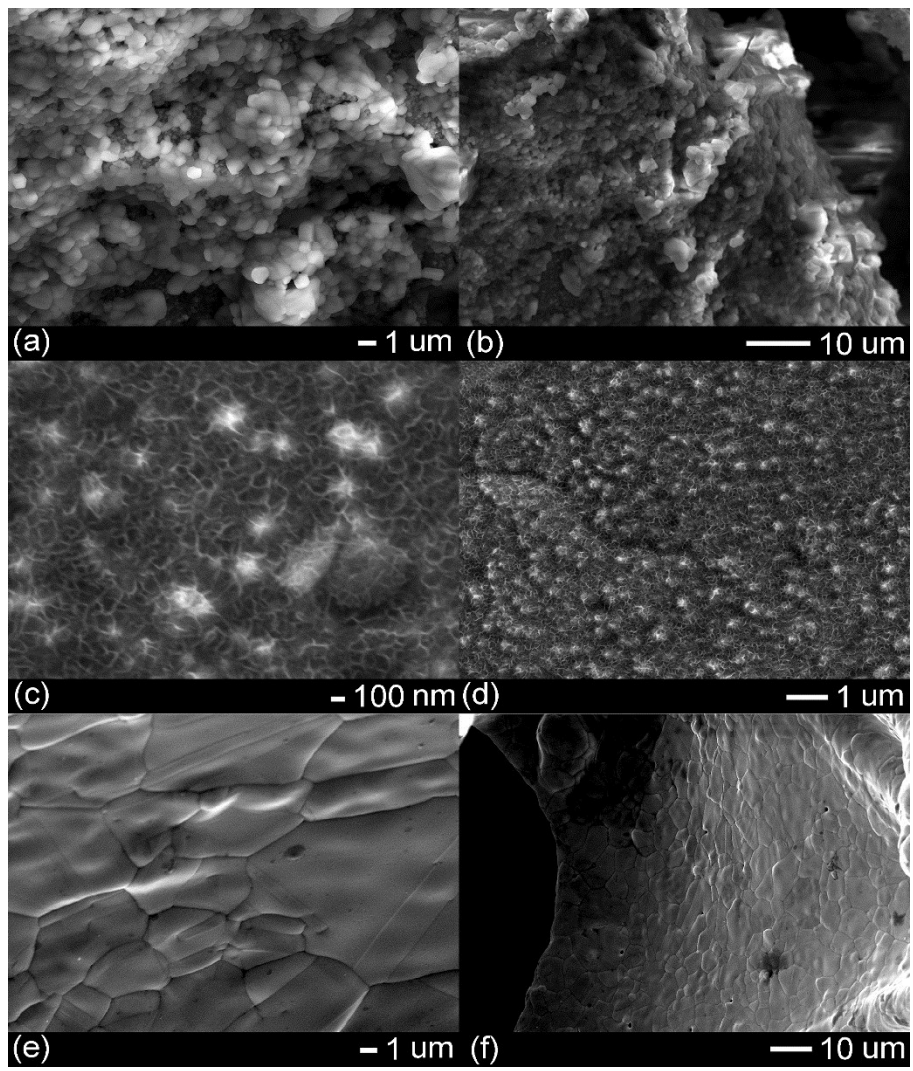


Fig. S3 SEM images of (a) and (b) Fe/NF, (c) and (d) Fe(OH)₃/NF, and (e) and (f) pristine NF.

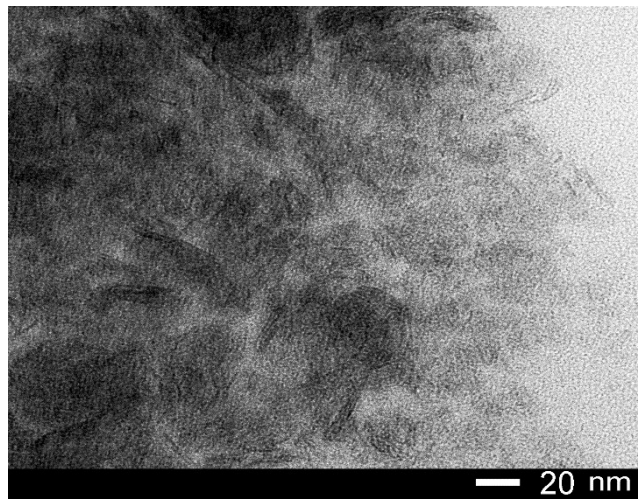


Fig. S4 TEM image of the as-prepared FeBO₃.

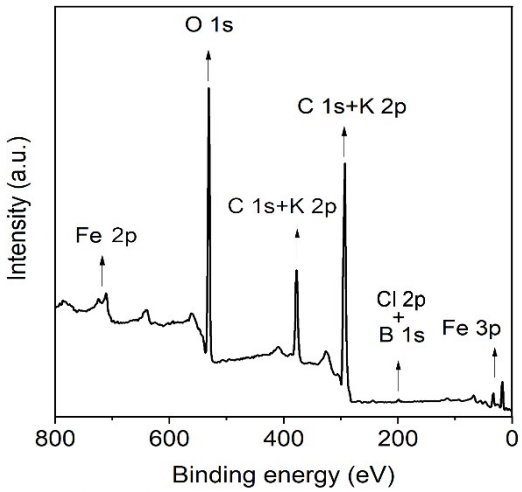


Fig. S5 XPS spectra overall survey of FeBO_3/NF .

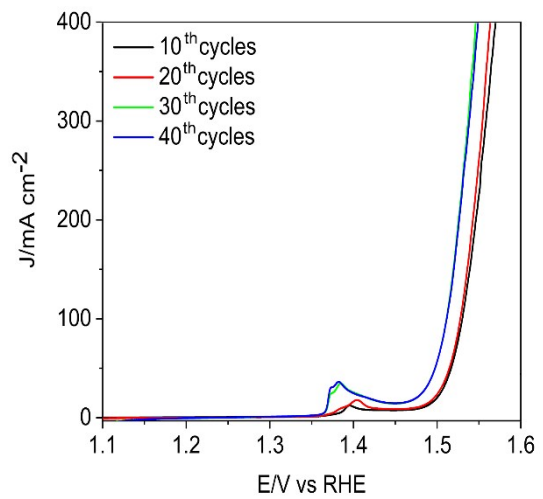


Fig. S6 Optimization for the number of dip-coating cycles to prepare FeBO₃/NF.

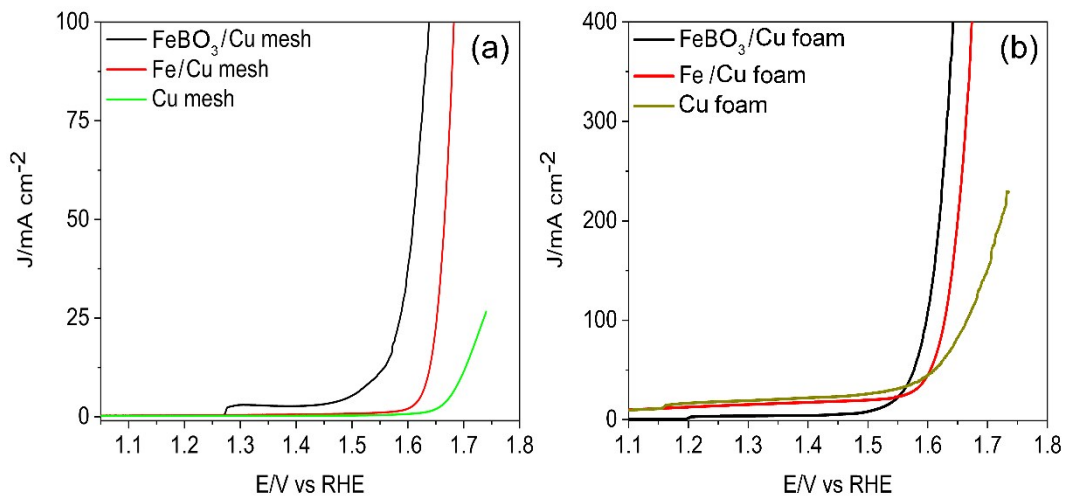


Fig. S7 OER polarization curves performed on (a) copper mesh and (b) copper foam as substrate at an iR correction level of 90%, scan rate of 5 mV s⁻¹, and in 1.0 M KOH.

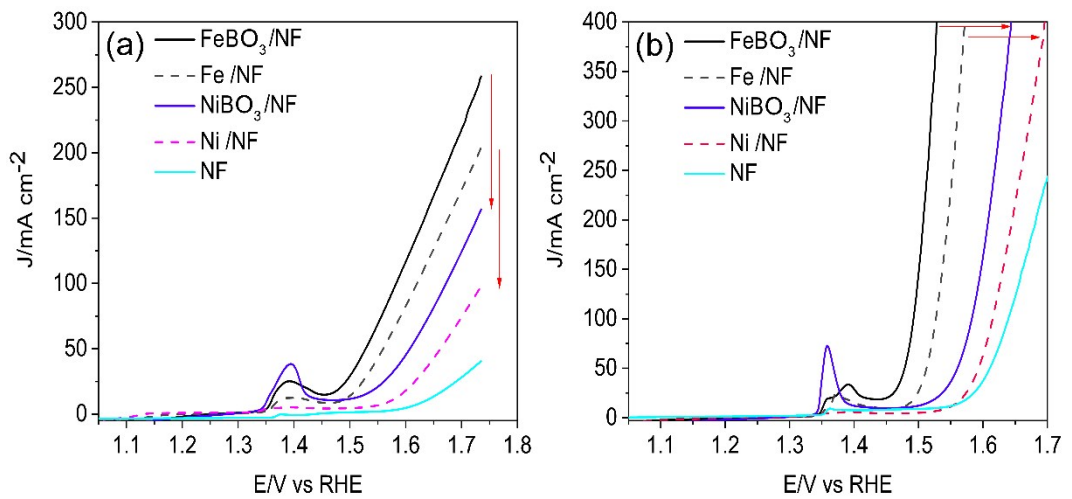


Fig. S8 Comparison of the OER polarization curves of FeBO₃/NF, Fe/NF, NiBO₃/NF, Ni/NF, and pristine NF samples (a) without and (b) with 90% iR compensation level, scan rate of 5 mV s^{-1} , and in 1.0 M KOH.

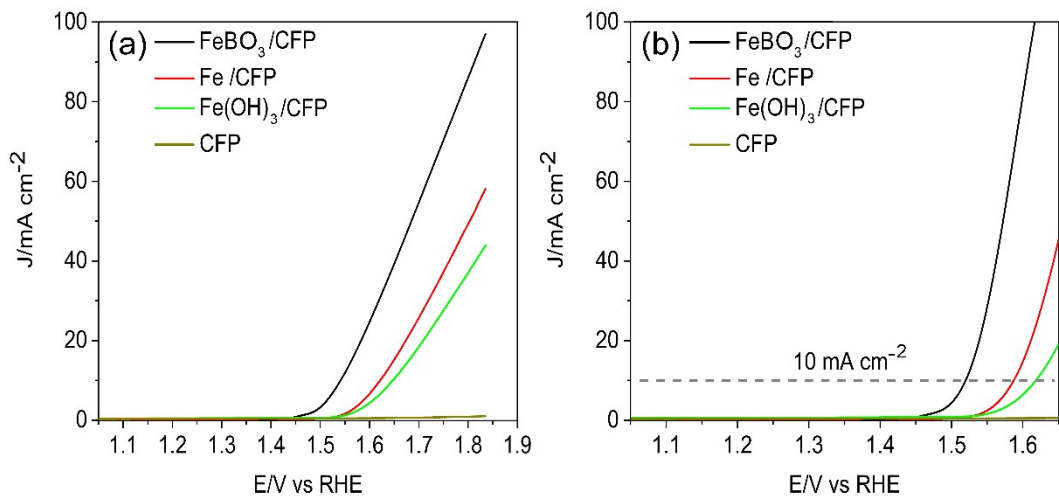


Fig. S9 Comparison of the OER polarization curves of scraped FeBO_3 , Fe , Fe(OH)_3 off the NF and loaded on inert CFP substrate (a) without and (b) with 90% iR compensation level, scan rate of 5 mV s^{-1} , and in 1.0 M KOH .

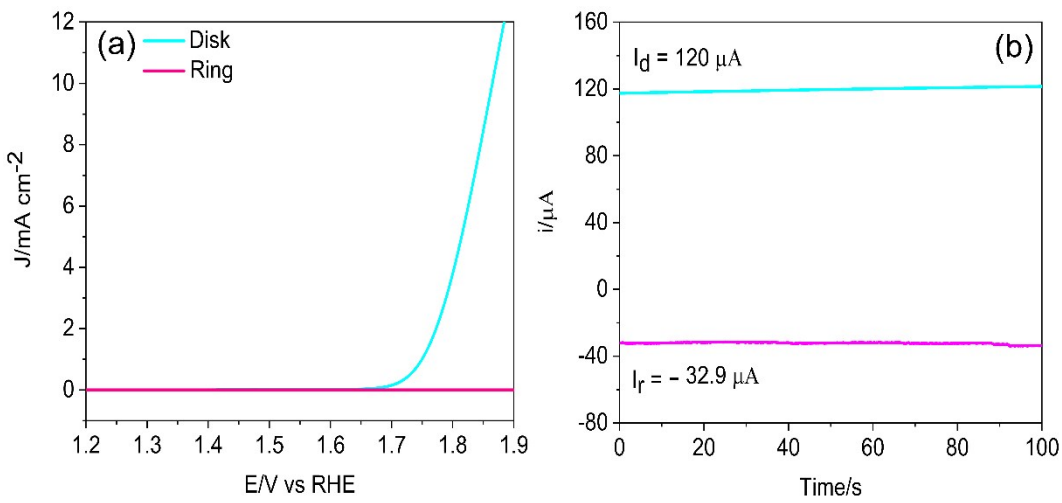


Fig. S10 (a) RRDE voltammogram for FeBO_3 ink loaded on RRDE (1600 rpm) in an O_2 -saturated 1.0 M KOH electrolyte with an applied potential of 1.5 V (vs RHE) at the ring electrode. (b) Comparison of disk and ring current responses obtained for FeBO_3 ink loaded on RRDE (1600 rpm) in an N_2 -saturated 1.0 M KOH electrolyte, with an applied potential of 0.4 V (vs RHE) at the ring and a constant current of $120 \mu\text{A}$ at the disk.

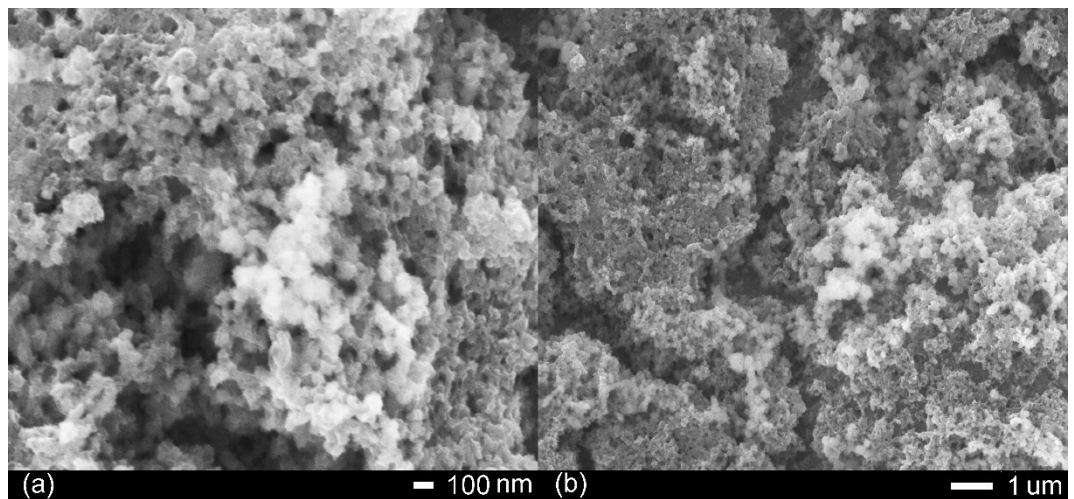


Fig. S11 (a) and (b) Post-OER SEM images of FeBO₃/NF.

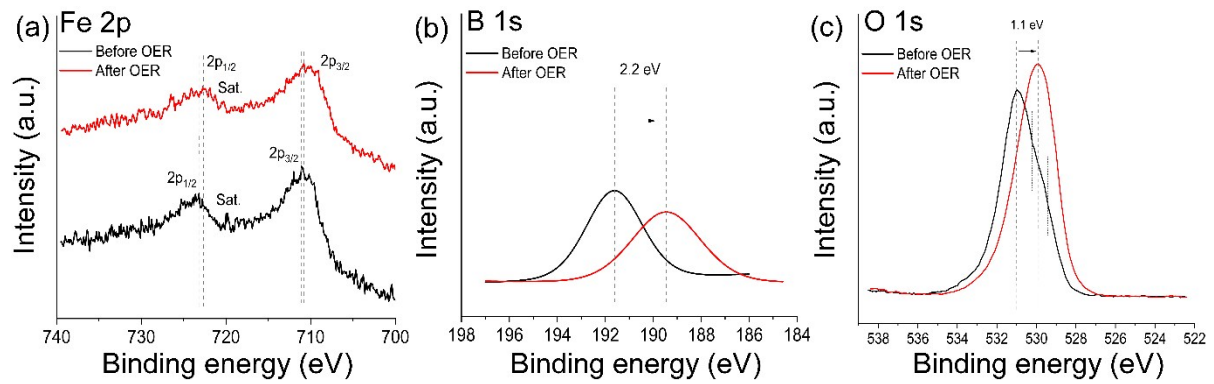


Fig. S12 Comparison of XPS profiles; (a) Fe 2p, (b) B 1s, and (c) O 1s high resolution spectra of FeBO₃/NF before and after OER.

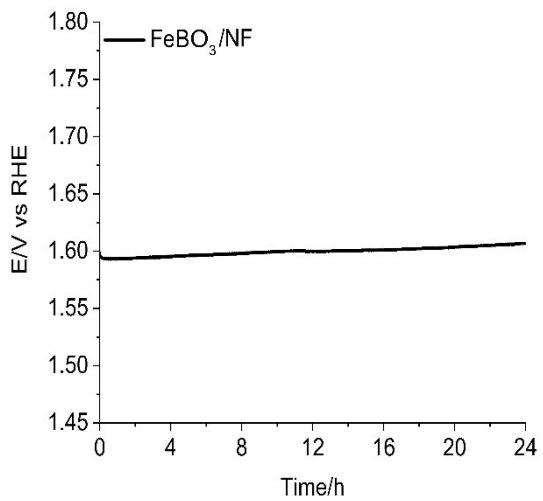


Fig. S13 Long-term stability test of FeBO_3/NF at a constant current density of 100 mA cm^{-2} .

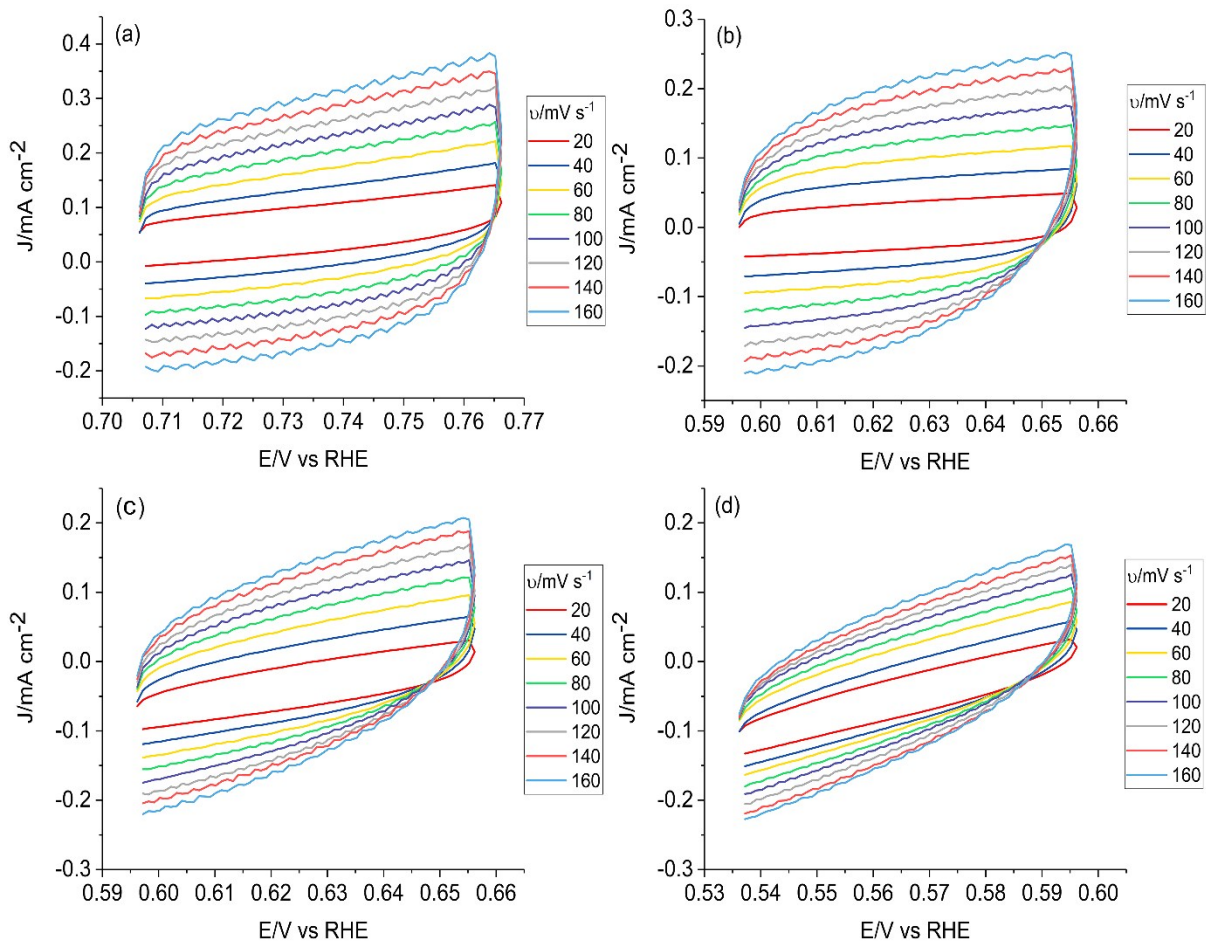


Fig. S14 Double-layer capacitance measurements of (a) FeBO_3/NF , (b) Fe/NF , (c) $\text{Fe(OH)}_3/\text{NF}$, and (d) pristine NF.

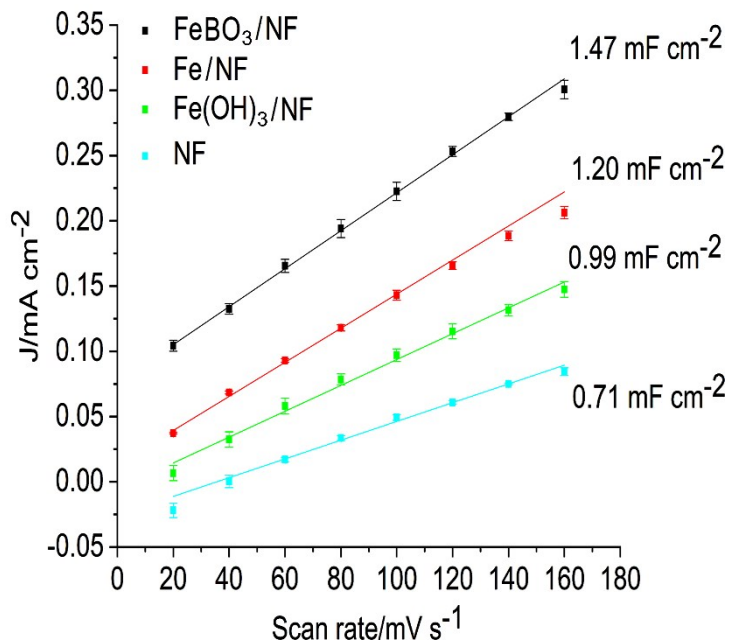


Fig. S15 Charging current density differences plotted against scan rates. The linear slopes were calculated based on the average value of three different measurements along with the standard deviation. The derived anodic slope was then considered equivalent to the double-layer capacitance, C_{DL} , and used to represent the ECSA.

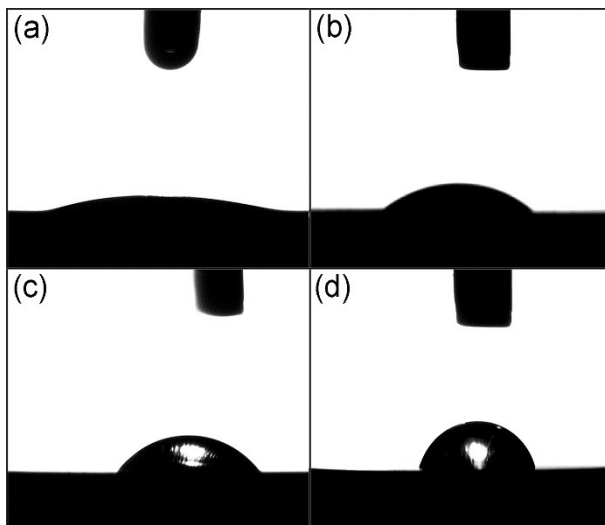


Fig. S16 Water droplet contact angle measurements on nickel foil deposited with (a) FeBO_3 , (b) Fe, (c) Fe(OH)_3 , respectively and (d) pristine nickel foil.

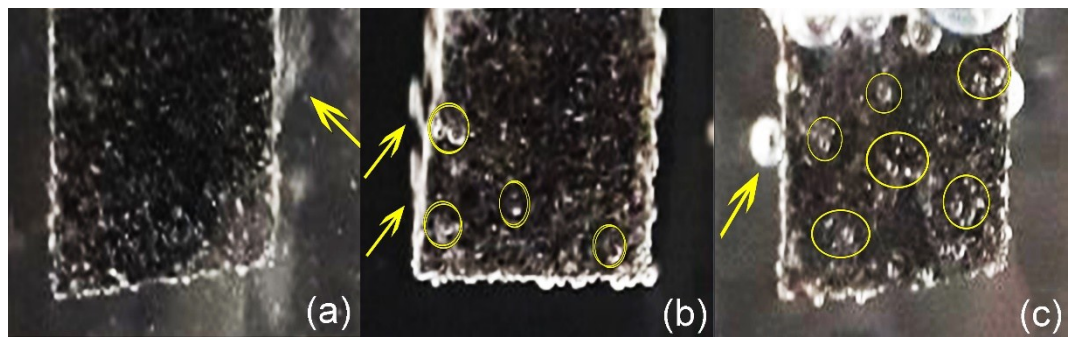


Fig. S17 Digital images of electrodes during a steady-state OER process upon applying 360 mV overpotential, (a) FeBO₃/NF, (b) Fe/NF, (c) Fe(OH)₃/NF.

Table S1 Comparison of OER behaviour of FeBO₃/NF electrode with those of state-of-the-art electrocatalysts at alkaline medium

Electrode	KOH Electrolyte concentration (M)	Overpotential@ 10 mA cm ⁻² (mV)	Tafel slope (mV dec ⁻¹)	Reference
FeBO ₃ /NF	1.0	232 ^a	46.3	This work
FePO ₄ /NF	1.0	215	28.0	S1
Ni _{0.9} Fe _{0.1} O _x /ITO ^b	1.0	336	30.0	S2
P-NiFe/NF	1.0	205	32.0	S3
NiFe LDH-NS-DG10/GC	1.0	210	52.0	S4
Ni:PO ₄ -Fe/NF	1.0	220	37.0	S5
NiFeO _x /IF	1.0	220	34.0	S6
NiFe LDH/NF	1.0	215	28.0	S7
NiFe LDH/NF	1.0	240	NA	S8
NiFe LDH/CNT	1.0	240	31.0	S9
α-Ni(OH) ₂ /GCDE ^c	0.1	331	42.0	S10
Ni _{0.53} Fe _{0.47} O _x /ITO	1.0	310	28.0	S11
Ni _{0.71} Fe _{0.29} (OH) _x /G ^d	0.1	296	58.0	S12
NiFe/NF	1.0	276 ^e	50.1	S13
NiSe/NF	1.0	270 ^f	64.0	S14
Ni-P/GCDE	1.0	300	64.0	S15
Ni ₂ P/GC	1.0	290	47.0	S16
NiFe-OH-PO ₄ /NF	1.0	249 ^g	41.8	S17
Ni ₃ S ₂ /NF	1.0	260	NA	S18
NiBO ₃ -NB/GCDE	1.0	302	52.0	S19
NiCo ₂ O ₄ -NiCoBO ₃ /CC ^h	1.0	270	62.0	S20

^{a,f,g}Overpotential at 20 mA cm⁻²

^bITO-coated glass electrode

^cGlassy carbon disk electrode

^dGraphite electrode

^eOverpotential at 50 mA cm⁻²

^hCarbon cloth electrode

Table S2 Simulated R_s and R_{ct} values for the electrocatalysts in this work via EIS spectra using the applied equivalent circuit

Sample	R_s (Ω)	R_Q (Ω)	R_{ct} (Ω)
FeBO ₃ /NF	3.043	0.042	1.062
Fe/NF	3.218	0.011	2.141
Fe(OH) ₃ /NF	3.556	0.012	2.716
RuO ₂ /NF	2.987	0.085	13.610
NF	3.642	0.040	18.960

References

- S1 D. Zhong, L. Liu, D. Li, C. Wei, Q. Wang, G. Hao, Q. Zhao and J. Li, *J. Mater. Chem. A*, 2017, 5, 18627–18633.
- S2 L. Trotochaud, J. K. Ranney, K. N. Williams and S. W. Boettcher, *J. Am. Chem. Soc.*, 2012, 134, 17253–17261.
- S3 F. S. Zhang, J. W. Wang, J. Luo, R. R. Liu, Z. M. Zhang, C. T. He and T. B. Lu, *Chem. Sci.*, 2018, 9, 1375–1384.
- S4 Y. Jia, L. Zhang, G. Gao, H. Chen, B. Wang, J. Zhou, M. T. Soo, M. Hong, X. Yan, G. Qian, J. Zou, A. Du, X. Yao, *Adv. Mater.*, 2017, 29, 1700017.
- S5 Y. Li and C. Zhao, *Chem. Mater.*, 2016, 28, 5659–5666.
- S6 J. Wang, L. Ji, S. Zuo and Z. Chen, *Adv. Energy Mater.*, 2017, 7, 1700107.
- S7 X. Lu and C. Zhao, *Nat. Commun.*, 2015, 6, 6616.
- S8 J. Luo, J. H. Im, M. T. Mayer, M. Schreier, M. K. Nazeeruddin, N. G. Park, S. D. Tilley, H. J. Fan and M. Grätzel, *Science*, 2014, 345, 1593–1566.
- S9 M. Gong, Y. Li, H. Wang, Y. Liang, J. Z. Wu, J. Zhou, J. Wang, T. Regier, F. Wei and H. Dai, *J. Am. Chem. Soc.*, 2013, 135, 8452–8455.
- S10 M. Gao, W. Sheng, Z. Zhuang, Q. Fang, S. Gu, J. Jiang and Yushan Yan, *J. Am. Chem. Soc.*, 2014, 136, 7077–7084.
- S11 J. Wang, L. L. Ji and Z. Chen, *ACS Catal.*, 2016, 6, 6987–6992.
- S12 Y. Q. Gao, X. Y. Liu and G. W. Yang, *Nanoscale*, 2016, 8, 5015–5023.
- S13 D. Guo, J. Qi, W. Zhang and R. Cao, *ChemSusChem.*, 2017, 10, 394–400.
- S14 C. Tang, N. Cheng, Z. Pu, W. Xing and X. Sun, *Angew. Chem. Int. Ed. Engl.*, 2015, 54, 9351–9355.
- S15 X. Y. Yu, Y. Feng, B. Guan, X. W. Lou and U. Paik, *Energy Environ. Sci.*, 2016, 9, 1246–1250.
- S16 L.A. Stern, L. Feng, F. Song and X. Hu, *Energy Environ. Sci.*, 2015, 8, 2347–2351.
- S17 Z. Lei, J. Bai, Y. Li, Z. Wang and C. Zhao, *ACS Appl. Mater. Interfaces*, 2017, 9, 35837–35846.
- S18 L. L. Feng, G. Yu, Y. Wu, G. D. Li, H. Li, Y. Sun, T. Asefa, W. Chen and X. Zou, *J. Am. Chem. Soc.*, 2015, 137, 14023–14026.
- S19 W. J. Jiang, S. Niu, T. Tang, Q. H. Zhang, X. Z. Liu, Y. Zhang, Y. Y. Chen, J. H. Li, L. Gu, L. J. Wan and J. S. Hu, *Angew. Chem. Int. Ed.*, 2017, 56, 6572–6577.
- S20 X. Ji, X. Ren, S. Hao, F. Xie, F. Qu, G. Du, A. M. Asiri and X. Sun, *Inorg. Chem. Front.*, 2017, 4, 1546–1550.